JOURNAL OF GEOPHYSICAL RESEARCH, VOL. 105, NO. B11, PAGES 25,891–25,907, NOVEMBER 10, 2000

# Fault rupture between dissimilar materials: Ill-posedness, regularization, and slip-pulse response

A. Cochard[1] and J. R. Rice

Department of Earth and Planetary Sciences and Division of Engineering and Applied Sciences, Harvard University, Cambridge, Massachusetts

**Abstract.** Faults often separate materials with different elastic properties. Nonuniform slip on such faults induces a change in normal stress. That suggests the possibility of self-sustained slip pulses [*Weertman*, 1980] propagating at the generalized Rayleigh wave speed even with a Coulomb constitutive law (i.e., with a constant coefficient of friction) and a remote driving shear stress that is arbitrarily less than the corresponding frictional strength. Following *Andrews and Ben-Zion* [1997] (ABZ), we study numerically, with a two-dimensional (2-D) plane strain geometry, the propagation of ruptures along such a dissimilar material interface. However, this problem has been shown to be ill-posed for a wide range of elastic material contrasts [*Renardy*, 1992; *Martins and Simões*, 1995; *Adams*, 1995]. *Ranjith and Rice* [2000] (RR) showed that when the generalized Rayleigh speed exists, as is the case for the material contrast studied by ABZ, the problem is ill-posed for all values of the coefficient of friction, $f$, whereas when it does not exist, the problem is ill-posed only for $f$ greater than a critical value. We illustrate the ill-posedness by showing that in the unstable range the numerical solutions do not converge through grid size reduction. By contrast, convergence is achieved in the stable range but, not unexpectedly, only dying pulses are then observed. RR showed that among other regularization procedures, use of an experimentally based law [*Prakash and Clifton*, 1993; *Prakash*, 1998], in which the shear strength in response to an abrupt change in normal stress evolves continuously with time or slip toward the corresponding Coulomb strength, provides a regularization. (Classical slip weakening or rate- and state-dependent constitutive laws having the same kind of abrupt response as Coulomb friction also do not regularize the problem.) Convergence through grid size reduction is then achieved in the otherwise ill-posed range. For sufficiently rapid shear strength evolution, self-sustained pulses are observed. When the generalized Rayleigh wave speed exists, they propagate essentially at that velocity and, in consistence with *Weertman*'s [1980] analysis, the propagation occurs only in one direction, which is that of slip in the more compliant medium. When the generalized Rayleigh wave speed does not exist, similar self-sustained pulses propagate at about the slower S wave speed and in the same direction. RR also suggested that for sufficiently high coefficient of friction, another kind of (less unstable) self-sustained pulses, propagating at a velocity close to the slower P wave speed and in the opposite direction, could also exist. We numerically verify that prediction.

## 1. Introduction

### 1.1. Material Contrasts in Crustal Rocks

Active faulting over geological times brings into contact materials that were originally far separated, thus being likely to have modestly different elastic properties. Indeed, such elastic contrasts across various faults have been observed by seismic reflection profiles [*Feng and McEvilly*, 1983] and by travel time tomography based on local earthquakes [e.g., *Eberhart-Phillips and Michael*, 1998; *Magistrale and Sanders*, 1995]. Estimates of the velocity contrasts range from a few percent to as high as $\sim$ 30%, depending on geographical location.

In addition to these contrasts across faults, some of the above studies were able to detect the presence, associated with the fault, of a narrow zone (of width ranging from a few tens of meters to a few thousands of meters) with seismic velocities lower than those in the surrounding rocks. These variations are thought to be due to the alteration of the material (increased porosity, presence of fluids, etc.) by repeated earthquakes. These low-velocity zones are best studied by analyzing the so-called head and trapped waves that are guided by such zones and whose features are strongly de-

[1] Now at Laboratoire de Géologie, École Normale Supérieure, Paris



Paper number 2000JB900230.
0148-0227/00/2000JB900230$09.00

pendent on the physical properties of the guide [e.g., *Ben-Zion*, 1998, and references therein]; inferred velocity contrasts may also be of the order of a few tens of percent [e.g., *Li et al.*, 1994]. Earthquakes can also occur at the interface of sedimentary layers, or in mining environments where, for example, rupture is expected at the interface between a dike and its more compliant surroundings [*York and Dede*, 1997], or in translatory rock bursting by unstable slip along the interface between a compliant coal seam and the stiffer floor or ceiling rock [*Lippmann*, 1987].

### 1.2. Bimaterials, Alteration of Normal Stress, and Slip Pulses

It is thus important to understand how such variations in material properties influence the dynamics of earthquake rupture. The simplest situation one can think of is that of a rupture along a planar bimaterial interface. It has long been recognized that the lack of symmetry in this case results, for the in-plane slip mode, in the normal stress being coupled to slip, which means that spatially nonuniform slip across a point causes a variation of normal stress at that same point. That is contrary to what happens, at least within the scope of linear elasticity, at the interface of two identical half-spaces. As it will turn out, this property alone leads to the emergence of a much richer phenomenology than rupture along a plane in a homogeneous continuum, not even to mention the multiple reflections on multiple boundaries that one would have to consider when dealing with more than two materials.

When the two materials on each side of a planar fault are identical, unstable slip is impossible if the interface is governed by the classical Coulomb law (i.e., with a single, constant coefficient of friction); it requires more elaborate friction laws for which, under constant normal stress, the friction stress at some point decreases as the slip displacement or slip velocity increases. By contrast, *Weertman* [1980] has shown analytically that the above mentioned coupling between slip and normal stress can lead to unstable slip. He thus suggested the possibility of a self-sustained propagation of a self-healing slip pulse along the frictional interface, even when the remote shear stress is less than the frictional strength. His pulse was shown to be promoted in one direction only. The situation Weertman considered occurs when the mismatch between the two materials is not too high, more precisely when the seismic properties of the two solids are such that the so-called generalized Rayleigh wave is defined. The velocity of propagation of the slip pulse is then the generalized Rayleigh wave speed. This particular type of wave, which has been first identified by *Weertman* [1963] and *Achenbach and Epstein* [1967], is a mode that propagates along the interface of two dissimilar materials, when these are assumed to slip freely (no friction) without opening; its amplitude decays with distance from the interface, much like for a Rayleigh or Stoneley wave. Like the ordinary Rayleigh wave, an interfacial wave propagating at the generalized Rayleigh wave speed leaves the shear stress unchanged at the interface; further, when the two materials are identical, the mode velocity reduces to the Rayleigh wave speed of that material. The generalized Rayleigh wave speed lies between the individual Rayleigh wave speed of each material and is slower than the slower S speed.

*Weertman* [1980] did not work out the exact solution of such a steady state traveling pulse but, independently, *Adams* [1998] fully derived the solution, and Adams' solution can be deduced easily from Weertman's developments [*Rice*, 1997]. It consists of any number of slipping zones, each one having an undetermined length along the fault (correspondingly, one may say that the risetime at a point is undetermined) all slipping at the same, well-defined sliding velocity and, as already mentioned, propagating at the generalized Rayleigh wave speed in a single direction. In particular, a very short risetime slip pulse is a solution.

This type of response reinforces the interest of bimaterial studies in seismology since it now seems well established that many earthquakes have risetimes much shorter than would be expected from classical crack models [*Heaton*, 1990]. Further, processes like the one just discussed, which allow earthquake rupture to propagate at overall shear stresses which are low compared to the friction threshold, provide a possible explanation of the apparent lack of observed heat flow from some major faults [*Lachenbruch and Sass*, 1980] as well as of the unexpectedly steep angle between the maximum principal compressive stress direction and the fault trace in some tectonic regions [*Zoback et al.*, 1987]. See the introduction of *Ben-Zion and Andrews* [1998] for a discussion of other unresolved problems that might be related to ruptures along bimaterial interfaces.

It is worth noting that there are other possible causes of alteration of normal stress across a fault zone during rupture, whose effects would add to those of material contrasts. Let us mention the influence of wave reflections from the free surface [*Oglesby et al.*, 1998] or the influence of nonplanar fault surfaces with step overs [*Harris and Day*, 1993] or kinks [*Bouchon and Streiff*, 1997]. Possibly more important is what might be a scaled down version of the above, namely, the effects of roughness at various scales [e.g., *Mora and Place*, 1994; *Lomnitz-Adler*, 1991]. Also, as will be elaborated further in section 5.4, it seems plausible that the unsymmetric state of stress generated by an in-plane rupture around a fault (compressional on one side, extensional on the other one), combined with a nonlinear response, may sometimes result in a homogeneous material mimicking bimaterial response. This could be the basis for the pulse-like ruptures, with local normal stress reduction and even fault opening, observed for fault propagation between foam rubber blocks by *Brune et al.* [1993] (see the introduction of *Andrews and Ben-Zion* [1997, and references therein] for a fuller discussion of the experiments by J. N. Brune and coworkers).

There are alternative explanations for short risetime slip pulses along a planar fault within a homogeneous medium. One of these requires more elaborate friction laws with a velocity-weakening component, as suggested by *Heaton* [1990] [*Cochard and Madariaga*, 1994; *Perrin et al.*, 1995; *Beeler and Tullis*, 1996; *Cochard and Madariaga*, 1996; *Zheng and Rice*, 1998]. Another explanation appeals to strong heterogeneities on the fault plane, which act as local barriers and generate arrest waves [*Day*, 1982; *Johnson*,

1990, 1992]. *Beroza and Mikumo* [1996] found such a heterogeneous numerical model, with nonuniform distribution of a (grid size dependent) stress excess to initiate slip and stress drop during slip, that could at the same time exhibit a very short risetime and reproduce the gross features of the seismograms generated by the 1984 Morgan Hill earthquake, which was the event in *Heaton*'s [1990] compilation with the shortest risetime. *Olsen et al.* [1997] constructed a similar, strongly heterogeneous model for short risetimes in the Landers 1992 earthquake.

### 1.3. Previous Numerical Work and Resolution Problems

Recently, using two-dimensional (2-D) in-plane strain finite difference simulations, *Andrews and Ben-Zion* [1997] (hereinafter referred to as ABZ) numerically addressed the problem of dynamic rupture along a planar material interface. They used a 20% material contrast in both seismic velocities and densities and a pure Coulomb law with constant coefficient of friction. As predicted by *Weertman* [1980], they found that self-healing slip pulses can propagate in a single direction, the direction of sliding in the softer medium, in a self-sustained way, when the initial shear stress is less than the initial strength (i.e., initial normal stress times the friction coefficient). The rupture velocity of this pulse is, within numerical uncertainties, in good agreement with the theoretical generalized Rayleigh wave speed. ABZ report numerical difficulties in resolving sharp features of the solution and discuss only the features that are common to the simulations obtained with two different resolutions. In particular, they find that the above so-called "Weertman" pulse splits into two pulses.

Subsequently, *Harris and Day* [1997] numerically studied, also with a finite difference method, a broader range of situations with material contrasts (still for a 2-D in-plane slip mode) in an attempt to better approach the observed natural diversity. They use a friction coefficient that includes slip dependence at the beginning of slip (slip weakening). In addition to the simpler case of a planar bimaterial interface, they simulated a low-velocity zone (LVZ) with parallel planar interfaces with a higher-velocity country rock. In that second case, the (planar) fault was chosen either in the middle of the LVZ (in which case, it is a plane of symmetry; hence no alteration of normal stress is expected) or at the interface between the LVZ and the country rock. They focus their attention on the rupture velocity, the shape of the slip function, and the normal stress variations. In no case did they find pulse-like ruptures nor unidirectional propagation. It is difficult to know why these findings differ from ABZ's since the physical situations that are simulated are never exactly identical to each other. The crack-versus-pulse discrepancy, however, is likely to originate in the nucleation procedure itself: in ABZ it consists of a pulse of increased then decreased pore fluid pressure (see details below), while it consists of a more classical kinematically imposed growing crack in the work of *Harris and Day* [1997]. One could think that the discrepancy could come from the different friction law used in the two studies. However, some tests were performed with slip weakening (the law *Harris and Day* [1997] used) and the ABZ nucleation process, and pulses were observed. By contrast, other tests done with the law used by ABZ (in a modified version of it so as to avoid ill-posedness, see section 1.4) and a different nucleation process, closer to the one used by *Harris and Day* [1997] (namely, an increased but not decreased pore fluid pressure) produced cracks. Of greater relevance here is the *Harris and Day* [1997] observation that, in particular in the case of the bimaterial simulations, they find unavoidable grid size dependence effects, no matter how refined their grid was. Like ABZ, though, they argue that features that are robust through grid refinements, like rupture velocities or crack-like characteristic of the rupture, are valid features of the solution.

However, as we will now discuss, at least part of the grid size dependence problems met by ABZ and *Harris and Day* [1997], and maybe also the difference between both studies, is likely to be due to the intrinsic ill-posed nature of the physical problem studied.

### 1.4. Ill-Posedness and Regularization

Previously, *Renardy* [1992] and *Martins and Simões* [1995] for the particular case of an elastic solid sliding against a rigid body and *Adams* [1995] for the general case of two elastic bodies have shown that sliding at a planar bimaterial interface under Coulomb friction is often not well-posed, that is, it does not possess any solution, as detailed in section 3.1. *Ranjith and Rice* [2000] have shown a connection between the existence of the generalized Rayleigh wave and the ill-posed nature of the problem. When the material pair is such that the generalized Rayleigh wave speed is defined, the problem is ill-posed for any value of the friction coefficient, whereas, when it is not defined, the problem remains ill-posed for values of the friction coefficient larger than a critical value $f_{\text{crit}}$.

In an extension of the ABZ study, in which they examined the influence of material contrasts, friction coefficients, and spatial heterogeneities on wrinkle-like propagation, *Ben-Zion and Andrews* [1998] suspected *Adams* [1995] instability to be responsible for the numerical problems that they had encountered. Indeed, we think that is exactly what happens, since the case studied by ABZ and at least some of the cases studied by *Harris and Day* [1997] and *Ben-Zion and Andrews* [1998] fall in the range (of seismological interest) in which the generalized Rayleigh wave speed is defined and are thus certainly ill-posed.

So we have to regularize the problem. We use an experimentally based friction law [*Prakash and Clifton*, 1993; *Prakash*, 1998] that smoothes into a continuous transition with time or slip the otherwise instantaneous variation of shear strength that would follow from an instantaneous variation in normal stress if the Coulomb law was used (see section 4.2). This law has been shown to provide a regularization by *Ranjith and Rice* [2000], who also note one other regularization approach [*Martins and Simões*, 1995; *Simões and Martins*, 1998]. Once regularized, the physical problem studied is of course no longer exactly the same as it was originally when the Coulomb law was used, so the natural question arises of which of the previously observed features remain at least

qualitatively valid. Addressing that is the main purpose of this paper. For example, it turns out that rupture still occurs as self-healing pulses but that the splitting of the pulse reported by ABZ does not survive the regularization, at least over time scales for which we have been able to do simulations.

## 2. Model Geometry

Following the work of ABZ, we study the elastodynamic propagation of ruptures along a fault that separates two semi-infinite elastic half-spaces of different material properties in the two-dimensional (2-D) plane strain geometry (Figure 1) with in-plane slip. We use and briefly outline here the spectral formulation of a boundary integral equation method developed by *Geubelle and Rice* [1995] and extended to dissimilar materials by *Breitenfeld and Geubelle* [1998].

The elastodynamic interactions between the fault surface and its elastic surroundings require that on the fault surface the traction components of stress $\tau_\alpha(x_1,t) = \sigma_{2\alpha}\,(\alpha = 1,2)$, which are necessarily continuous on $x_2 = 0$ (here $\sigma_{\beta\alpha}$ is the stress tensor), and the resulting displacements $u_\alpha^\pm$ along $x_2 = 0$ be related by

$$\begin{aligned}\tau_1 &= \tau_1^0(x_1,t) \mp \frac{\mu^\pm}{c_s^\pm}\frac{\partial u_1^\pm(x_1,t)}{\partial t} + \phi_1^\pm(x_1,t)\\ \tau_2 &= \tau_2^0(x_1,t) \mp \frac{c_p^\pm}{c_s^\pm}\frac{\mu^\pm}{c_s^\pm}\frac{\partial u_2^\pm(x_1,t)}{\partial t} + \phi_2^\pm(x_1,t)\end{aligned} \tag{1}$$

for which material properties in $x_2 > 0$ (respectively $x_2 < 0$) are denoted by a plus (respectively minus) superscript, and where $c_s$ and $c_p$ are the shear and dilatational wave speed, respectively (see Figure 1). The $\tau_\alpha^0(x_1,t)$ are the externally applied stresses that would act in the absence of any slip or opening. The terms proportional to $\partial u_\alpha^\pm/\partial t$, often called the radiation damping terms, show the instantaneous variation of slip velocities due to change in stresses. The functionals $\phi_\alpha^\pm$ represent the wave-mediated stress contributions from the rest of the fault due to prior displacement history along the interface. Further details about the functionals and the numerical procedure are described in Appendix A.

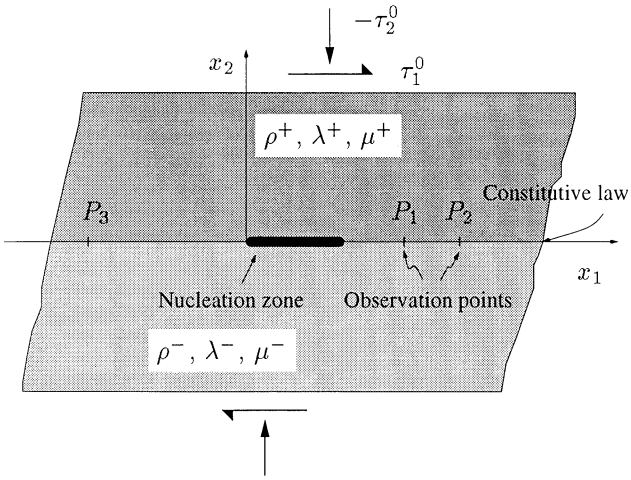


**Figure 1.** Two-dimensional in-plane slip model, in which ruptures are simulated along along the planar interface that separates two semi-infinite half-spaces of different elastic properties. Owing to material dissimilarity, instability may develop in this model even with the Coulomb friction law. Following *Andrews and Ben-Zion* [1997], ruptures are nucleated by an artificial localized spatiotemporal distribution of elevated pore pressure.

Following ABZ, the simulations are done as follows: we start with uniform normal and shear stresses distributions such that the media would remain at rest, i.e., $|\tau_1^0| < f|\tau_2^0|$ ($\tau_2^0 < 0$), where $f$ is the coefficient of friction. Then we artificially nucleate an event by increasing the pore fluid pressure, i.e., decreasing the effective normal stress $|\tau_2^0|$, in a limited space-time region (see Figure 1). Finally, we impose some constitutive law at the interface, which we discuss in section 3.

## 3. Ill-Posed Nature of the Problem With Classical Coulomb Friction

With identical materials, Coulomb friction, and a uniform initial stress along the $x_1$ axis in Figure 1 that is less than the frictional strength ($|\tau_1^0| < f|\tau_2^0|$), no matter how vigorously an event is initiated in the nucleation zone, it ultimately dies. With dissimilar materials. and following ABZ, one would ideally wish to use Coulomb friction, i.e., constant coefficient of friction, to study the instability due to material contrast independently from other, more classical sources of instabilities (e.g., rate-dependent friction). We emphasize that we are not considering a static/kinetic friction, which is sometimes referred to as "Coulomb" friction but is, in fact, a particular case of rate-dependent friction.

### 3.1. Harmonic Perturbation of Steady Sliding

As remarked, *Renardy* [1992] and *Martins and Simões* [1995] for the elastic/rigid case and *Adams* [1995] for the general elastic/elastic case have shown that such a problem is often not well-posed. (Note that Adams did not mention ill-posedness, which is only implicit in his results.) They all considered the same model of two semi-infinite half-spaces (as in Figure 1 but without the nucleation zone) sliding past one another at a constant velocity $V = \dot{u}_1^+ - \dot{u}_1^-$ with constant traction stresses $\tau_1^0 = -f\tau_2^0$ and looked for perturbed solutions of the elastodynamic equations with an $\exp(ikx_1)$ space dependence. We generated such solutions numerically (Figure 2) by supposing that the shear stress $\tau_1^0$ is perturbed by the harmonic quantity

$$\Delta\tau_1^0(x_1,t) = Q(t)e^{ikx_1}\,, \tag{2}$$

$Q(t)$ being arbitrary in general but taken as a step function in those illustrations. *Adams* [1995] looked for such $\exp(ikx_1)$ solutions and found propagating slip rate perturbation modes of the form

$$\Delta V(x_1,t) \propto e^{\Lambda t}e^{ikx_1} = e^{ik(x_1-ct)}e^{a|k|t}\,, \tag{3}$$

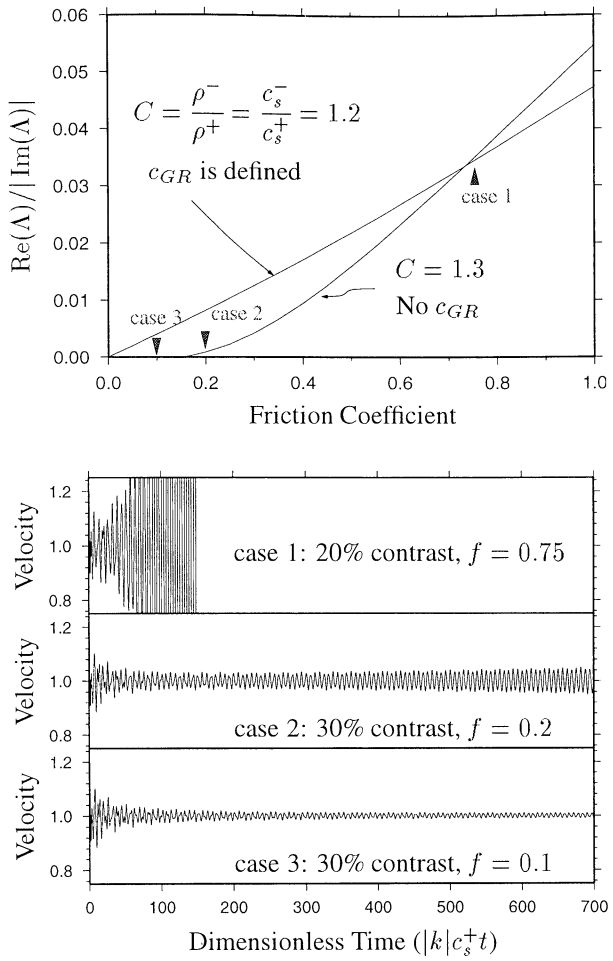


**Figure 2.** (top) Measure of instability, i.e., rate of exponential growth of velocity following a harmonic perturbation of the loading stress to the two half-spaces of Figure 1 in steady sliding under Coulomb friction (see equation (3)). For a 20% material contrast the generalized Rayleigh wave speed is defined. In such cases, there is instability for all values of the coefficient of friction. When the generalized Rayleigh wave speed is not defined, as is the case for a 30% material contrast, there is a transition. (bottom) Numerical illustration of the velocity (normalized by the unperturbed velocity) as a function of normalized time at a point, in response to a Heaviside-in-time perturbation, for the three representative cases noted at the top (20% contrast with $f = 0.75$; 30% contrast with $f = 0.1$ and $f = 0.2$). Exponential growth with normalized rate independent of mode number $k$ (as is the case here) implies ill-posedness for general problems (see text).

with $\Lambda = a|k| - \mathrm{i}ck$, with $a$ and the propagation speed $c$ being real and independent of the wavenumber $k$ and with $a > 0$ for a broad range of friction coefficients and material contrasts.

For such $a > 0$ cases, all wavelengths in the slip response are unstable, and the growth rate of the instability is inversely proportional to the wavelength. Thus the solution given by summing such modes,

$$\Delta V(x_1, t) = \frac{1}{2\pi} \int_{-\infty}^{+\infty} \Delta V_0(k, 0) e^{a|k|t} e^{\mathrm{i}k(x_1 - ct)} dk \ , \quad (4)$$

fails to exist (it diverges by oscillation at large $k$ for any nonzero $x_1 - ct$) for all time $t > 0$ whenever we consider a generic perturbation for which the Fourier transform $\Delta V_0(k, 0)$ of the component in that unstable mode decays less rapidly with $k$ than exponential at large $|k|$. Such a problem is said to be ill-posed. Note that this is not contradictory to the existence of the *Adams* [1998] steady pulse discussed previously, since this pulse is supposed to exist since $t = -\infty$ and hence has not been created by any perturbation of shear stress $\tau_1^0$, which is uniform along the interface in that case. However, the steady pulse is expected to be unstable.

We show in Figure 2 (top) how the *Adams* [1995] instability varies with friction coefficient for two representative cases of material contrasts, both with identical Poisson ratios equal to $1/4$: one for a 20% contrast in wave velocities and densities, i.e., $C = \rho^-/\rho^+ = c_s^-/c_s^+ = 1.2$ (a generalized Rayleigh wave exists in this case) and one for a 30% contrast, i.e., $C = 1.3$ (no generalized Rayleigh wave exist). One can see that for a 30% contrast the transition value is $f_{\text{crit}} \approx 0.15$. (Note that $\Lambda$ here differs from $\Lambda$ of *Adams* [1995], who used a nondimensionalized quantity; however, the quantity represented on the y axis in Figure 2 is the same as Adams', as the dimensionalizing factors cancel out.) We further illustrate instability by showing in Figure 2 (bottom) the velocity at one point of our numerical model when a harmonic stress perturbation is introduced at time 0 on the steady sliding system (i.e., $Q(t)$ in equation (2) is the Heaviside function). This is also shown to demonstrate the robustness of our numerical scheme. Even when regularization is introduced (section 4), the underlying physical instability appears extremely strong, and the numerical resolution remains very challenging.

### 3.2. Numerical Illustration of Ill-Posedness in the Unstable Range

We now move to the simulations of realistic cases corresponding to various cases of Figure 2. In this section we precisely mimic the conditions of one of ABZ studies (corresponding to their Figures 9-12). We have a 20% contrast with friction coefficient $f = 0.75$ (corresponding to case 1 in Figure 2). The initial shear stress is equal to 93.3% of the frictional strength. An event is initiated by superposing some smoothly rising then decaying fluid pressure to the initial stress $\tau_2^0$ inside the nucleation region in the $x_1 - t$ plane. The mathematical details are copied from ABZ and are recalled in Appendix B. We will focus on response at locations $P_1$ and $P_2$ at $x_1 = 99.9$ m and 134.9 m, respectively, the leftmost side of the roughly 60 m nucleation region being located at the origin (see Figure 1); later we will also consider $P_3$ at $x_1 = -100.7$ m.

The shear strength $\tau_1^s > 0$ consistent with a symmetric Coulomb friction is given by

$$\tau_1^s = f \max(0, -\tau_2) \ , \quad (5)$$

where $f$ is the friction coefficient and $\tau_2$ is the effective normal stress (incorporates the externally imposed fluid pressure). When velocity is zero, sliding is initiated when $|\tau_1|$

becomes equal to $\tau_1^s$. During sliding, $|\tau_1|$ remains equal to $\tau_1^s$ with the sign of $V$ being the same as that of $\tau_1$ ($\tau_1 V \geq 0$). Opening, which could occur in cases where $\tau_2 > 0$, is precluded in the simulations presented in this paper. Except inside the nucleation region, for the time extent of simulations presented, we have encountered this situation only in the pathological case that we now discuss (and very late in the simulation).

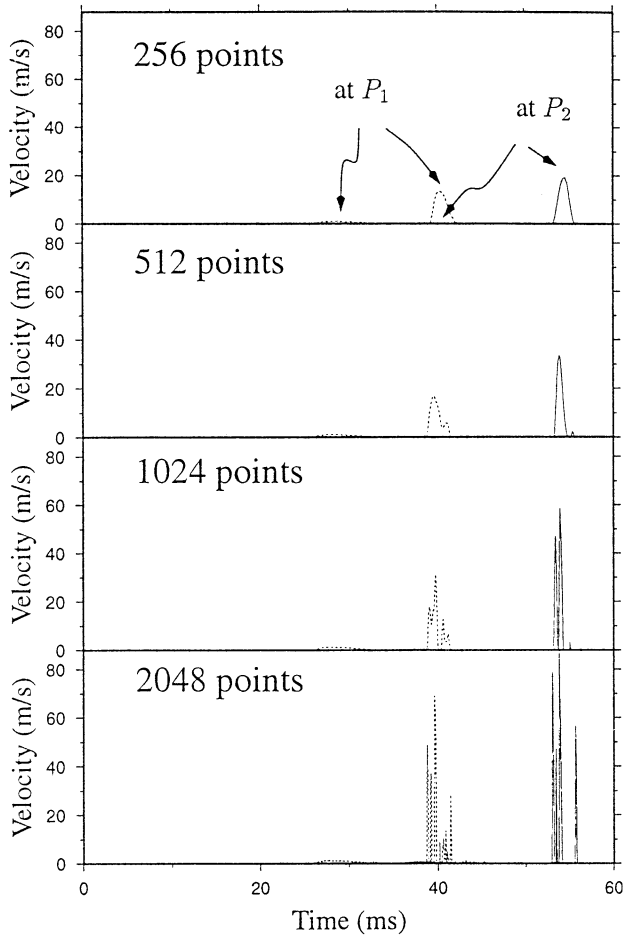


**Figure 3.** Exact mimic of *Andrews and Ben-Zion*'s [1997] conditions showing the slip velocity at two points of the fault plane, following an artificially nucleated rupture. The conditions are those of the unstable case 1 of Figure 2, of a 20% material contrast with Coulomb friction. From top to bottom we show four different levels of increasing grid refinement, each time decreasing the grid size by a factor of 2. Convergence of the solution through increasing resolution is not obtained, which illustrates ill-posedness, as discussed in the text. (Material properties are Poisson ratios $\nu^- = \nu^+ = 1/4$, $C = \rho^-/\rho^+ = c_s^-/c_s^+ = 1.2$, $\mu^- = 30$ GPa, $c_s^- = 3$ km/s. Initial conditions are $\tau_2^0 = -100$ MPa, $\tau_1^0 = 0.933 f|\tau_2^0|$. Nucleation characteristics of the spatiotemporal pore fluid distribution are (see Appendix B) $P_0 = |\tau_2^0|$, $a_{\text{ell}} = 10$ m, $b_{\text{ell}} = 60$ m (which corresponds to a spatial nucleation extension given by $\sqrt{a_{\text{ell}}^2 + b_{\text{ell}}^2} \approx 60.8$ m) and $v_{\text{ell}} = 2475$ m/s. The friction coefficient is $f = 0.75$. Purely numerical parameters are replication length $\lambda = 437.2$ m, Courant parameter $h = \max(c_s^+, c_s^-)\Delta t/\Delta x_1 = 0.4$ (see Appendix A), and the number of points $N$ as indicated in the figure.)

We represent in Figure 3 the sliding velocity at points $P_1$ and $P_2$ (which should be compared to ABZ's Figure 11, in which they used dimensionless variables) for different resolutions, that is, the replication length $\lambda$ in the numerical method is kept constant while the number of points used to discretize $\lambda$, corresponding to the number of terms in the Fourier series (see equation (A3)), is increased as indicated ($\Delta x_1 = \lambda/N$). There is no hint of convergence through grid size and time step reduction (we keep a constant value for the Courant parameter $h = \max(c_s^+, c_s^-)\Delta t/\Delta x_1$; see Appendix A). Rather, we see that the maximum velocity reached becomes increasingly larger for increasing resolution. Further, this pulse splits into a swarm of narrower pulses. (Like ABZ we find here that the "average" pulse velocity is nearly that of the generalized Rayleigh wave speed, but this is not significant: If we could further increase the resolution, as has been checked with these resolutions but with a higher modal growth rate, the figure would become full of one-point spikes and no velocity could be measured. Even before this state of total chaos, one observes that the pulse propagating at the slower P wave velocity, that is, the one that arrives at $P_1$ at time $\sim 25$ ms and which seems well resolved, begins to resemble the noisy pulse observed here.) ABZ did simulate the problem with two different resolutions. They found a splitting into two pulses with both resolutions which led them argue that this was "a believable feature of the results" (p. 563). Later, *Ben-Zion and Andrews* [1998] suspected *Adams*'s [1995] instability to be responsible for this feature, but it was not clear at that time that the set of physical parameters used were, indeed, in the Adams' unstable range, as we showed in section 3.1.

Now, in the light of *Adams*'s [1995] instability, one can interpret heuristically the numerical results of Figure 2: When increasing resolution, one is effectively injecting higher and higher modes (higher $k$) in the numerical solution. This is fully apparent with the numerical method we use which makes use of summations of Fourier modes (see equation (A3)), but is the same, although less explicit, for any other numerical method and in particular for the finite difference method that ABZ used. Hence the exponential growth (with dependence on $k$) will be visible earlier and earlier in the simulation or, conversely, have stronger consequences at a given time, which is observed in Figure 3. With the results obtained with the lower resolution we see that one can get apparently stable results even for an ill-posed problem, just because the instability has not become visible yet. This is a likely explanation why most of the results presented by *Harris and Day* [1997] are apparently stable numerically in spite of the instability mechanism. Also, and contrary to ABZ, *Harris and Day* [1997] used a numerical viscosity in their finite difference scheme, which is likely to further delay the appearance of the instability (D. J. Andrews and S. Day, personal communication, 2000). They studied the same kind of bimaterial (or trimaterial) systems with a slip weakening friction with strength $\tau_1^s$ at a given slip proportional to $-\tau_2$, for which the problem is also ill-posed, as discussed in section 4.

If one wants to persist using classical Coulomb friction and to have solutions exist, one must move outside the ill-posed range, which we now discuss.

### 3.3. Moving Outside the Unstable Range

We performed the same kind of simulation as shown in Figure 3, still with Coulomb law, but with a set of physical parameters for which the problem is no longer ill-posed: a 30% material contrast and a friction coefficient $f = 0.1$, corresponding to case 3 in Figure 2. As shown in Figure 2, this problem is Adams stable.

Again, the sliding velocity at points $P_1$ and $P_2$ is shown in Figure 4 with several numerical resolutions. The first obvious observation is that the results converge to a seemingly unique solution. Second, the propagation velocities of the pulses are close to those of the slower P and S waves (remember that the generalized Rayleigh wave speed is not defined in this case). More precisely, the velocity of the faster pulse is $V_r = 3628 \pm 12$ m/s at $P_1$ and $V_r = 3421 \pm 10$ m/s at $P_2$ (thus slowing down), while that of the slower pulse is $V_r = 2279 \pm 4$ m/s at $P_1$ and $V_r = 2286 \pm 4$ m/s at $P_2$ (the uncertainties coming for the finiteness of the numerical time step), while the slower P and S wave speeds are $c_p^+ = 3997.0$ m/s and $c_s^+ = 2307.7$ m/s, respectively. As can be seen in Figure 4, both pulses are dying. As is natural to expect, this is a generic feature of all simulations that we did in this Adams stable range. Simulations performed with the same material contrast (30%), but in the Adams unstable range (e.g., $f = 0.2 > f_{\text{crit}}$, as case 2 in Figure 2), show the same kind of grid dependence as in Figure 3.

## 4. Regularization of Ill-Posedness and the Simplified Prakash-Clifton Law

We will use an experimentally based constitutive law [*Prakash and Clifton*, 1993; *Prakash*, 1998] that has been shown to provide a regularization to the previously discussed ill-posedness [*Ranjith and Rice*, 2000].

### 4.1. Friction Under Variable Normal Stress: Experimental and Theoretical Background

It is very intuitive that since the ill-posedness nature of the problem originates from alteration of normal stress, the variation of normal stress has to be taken into account in a proper constitutive law. In particular, classical slip weakening or rate- and state-dependent constitutive laws, with strength level proportional to local normal stress, times a function of slip or slip rate and state, do not provide a regularization. This is trivial for slip weakening since it is then equivalent to Coulomb friction as soon as the slip-weakening distance is overcome. For a given dissimilar material problem, use of slip weakening simply delays the time of occurrence of obvious noisy numerical results. Conversely, for a given time, one can obtain seemingly stable numerical results with a smaller grid size. This may be part of the reason why most of *Harris and Day*'s [1997] results appear stable even in the ill-posed range. The same reasoning applies for classical rate- and state-dependent constitutive laws. Several levels of grid size reductions might look stable, but they are not comparable with each other, and in any event, numerical noise of the kind shown in Figure 3 will always reappear through further grid reduction, as we have checked in our simulations with slip weakening and rate- and state-dependent constitutive laws.

*Martins and Simões* [1995] and *Simões and Martins* [1998] proposed several types of law which achieve regularization. In one which is able to deal with the case of two elastic half-spaces without opening, the usual dependence on normal stress in the Coulomb law is replaced by a dependence on normal stress averaged over some small finite area. However, such a law would not, for example, be consistent with the experimental results of *Prakash and Clifton* [1993] and *Prakash* [1998] now discussed.

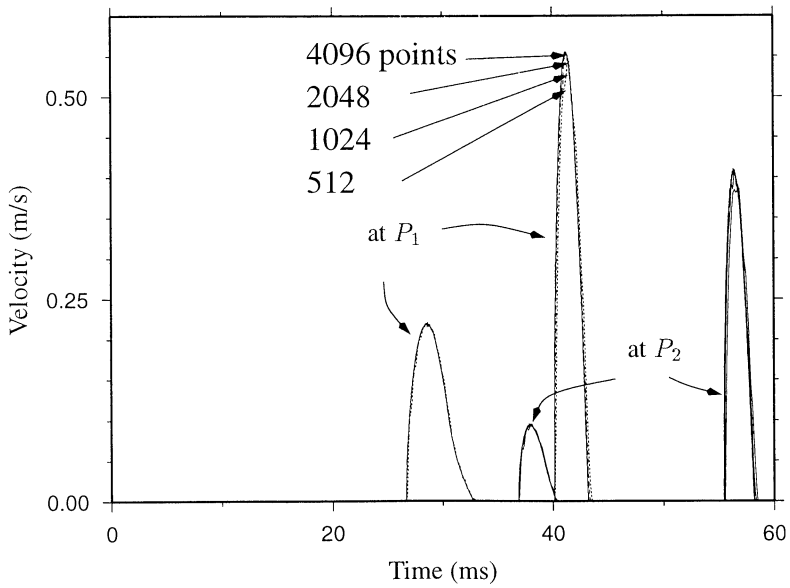


**Figure 4.** Same parameters as in Figure 3 but for a 30% material contrast ($C = 1.3$) with a friction coefficient $f = 0.1$, i.e., below the critical value. This corresponds to case 3 in Figure 2. The problem is not ill-posed, and the numerical solution converges through grid size reduction. However, the pulse is not self-sustained.

These experiments involved oblique shock impacts between hard metal and cutting tool plates that induce relative sliding at high relative velocities of the order of meters per second. The first reflected wave from the back of the target plate produces a very abrupt, effectively instantaneous step reduction in normal stress at the interface. Using the equations of one-dimensional wave propagation (which apply for the part of their experiment for which results are reported) and further accurately monitoring the displacements at the back face of the target plate, these authors were able to infer slip rate and stresses at the interface. These experiments are conceptually very simple in that, unlike most friction experiments, there is no apparatus stiffness to take into account; in that respect, they are easier to interpret.

The results suggest that there is no instantaneous change of shear strength, but rather a gradual change which occurs over a few microns of sliding or about $0.1$ $\mu$s in time (see Figure 5). They can be interpreted in the framework of rate- and state-dependent friction, in which shear strength is regarded as a property of the current population of asperity contacts, and of their lifetimes, if we assume that it is only with ongoing slip or time that the population, and therefore the shear strength, can be altered. That is, there is no instantaneous dependence of shear strength on normal stress but only an effect which has a fading memory dependence on recent normal stress history. Note that with the regularizing friction law of *Martins and Simões* [1995] and *Simões and Martins* [1998] discussed above, an abrupt decrease in shear strength simultaneous with the decrease in normal stress would have been predicted since $\tau_1$ is then rewritten as $f$ times the average of $-\tau_2$ over a small finite area and, owing to the experimental design, $\tau_2$ is approximately uniform over the entire macroscopic sliding surface.

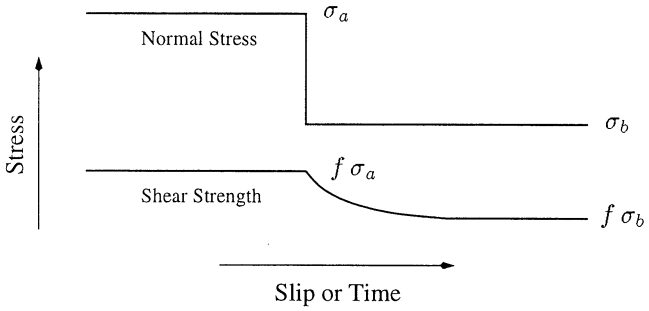


**Figure 5.** A simplified Prakash-Clifton law. It is necessary to incorporate a proper response to alteration of normal stress in order to regularize ill-posedness. In particular, classical slip-weakening or rate- and state-dependent constitutive laws with instantaneous response to change in local normal stress will not be appropriate. The bottom curve is a schematic illustration of the response of the interface following an abrupt change in normal stress (top curve) with the experimentally based *Prakash and Clifton* [1993] and *Prakash* [1998] constitutive law that we use to regularize the problem; strength evolves toward the corresponding Coulomb strength with constant coefficient of friction $f$. Exact evolution law used is described by equation (7).

However, earlier as well as recent studies on rock samples [*Linker and Dieterich*, 1992; *Richardson and Marone*, 1999] at slip rates of order $1$ $\mu$m/s imposed changes in normal stress during slip. Those workers found that there was a partial sudden change in the shear strength, followed by a gradual accumulation of the full effect of the altered normal stress over increasing slip and time. Since the shock experiments study the normal stress alteration over a much shorter timescale, we believe that it is appropriate, before more experimental studies can resolve this issue, to use their result here, and to interpret the "sudden" change of shear strength of *Linker and Dieterich* [1992] as a possible feature of the slow creep slippage range that they studied, or possibly an effect of their less abrupt change in time (compared with the shock experiments), which may have mapped memory effects into an apparent instantaneous effect.

*Linker and Dieterich* [1992] have a parameter $\alpha$ in their proposed constitutive law which they consider as a constant. However, we observe (see also H. Perfettini et al. (Fault response induced by time-dependent fluctuations of the normal loading, submitted to *Journal of Geophysical Research*, 2000)) that if we take $\alpha$ as nonconstant, and specifically set $\alpha = f = |\tau_1|/|\tau_2|$ (although this does not seem to be supported by their results), then the *Linker and Dieterich* [1992] law predicts no change of $|\tau_1|$ for an abrupt change of $\tau_2$ at a given slip rate. Recently, *Bureau et al.* [2000] did PMMA-on-PMMA friction experiments with variable normal stress, and reported results that cannot be interpreted in terms of the *Linker and Dieterich* [1992] law.

### 4.2. A Simplified Prakash-Clifton Constitutive Law

The constitutive law proposed by *Prakash and Clifton* [1993] and *Prakash* [1998] to interpret their experimental results includes the classical rate and state dependence at constant normal stress. As we want to concentrate on the instability mechanism specific to bimaterials, we first consider a simpler form:

$$\dot{\tau}_1 = -(V/L)(\tau_1 + f\tau_2) \tag{6}$$

(assuming $V, L > 0$), for which response tends to evolve toward Coulomb friction response, $\tau_1 \to -f\tau_2$, through a characteristic slip distance $L$ (see Figure 5).

By using the same kind of modal analysis as that used to rederive ill-posedness with Coulomb friction (section 3.1), *Ranjith and Rice* [2000] were able to show that this simplified form does provide regularization. More precisely, they show that for conditions under which the generalized Rayleigh wave speed exists, even if all wavelengths are still unstable with this friction law, the rate of exponential growth now depends on the wavenumber $k$ in a way which insures a finite energy integral over all excited modes for all times so that the stability problem is now well-posed. For conditions under which the generalized Rayleigh wave speed does not exist, *Ranjith and Rice* [2000] found generic stability at sufficiently small wavelengths (i.e., sufficiently large $k$) for all values of $f$, proving well-posedness in that case. They

also note that well-posedness would result if (again, assuming $V > 0$) the term $V/L$ in (6) was replaced by a positive constant or by a term of form $\hat{a} + \hat{b}V$ where both $\hat{a}$ and $\hat{b}$ are non negative and at least one is nonzero.

Numerical tests of the form shown in section 3.1 are consistent with this analysis. The same kind of behavior as shown in Figure 2 (bottom) is observed, i.e., a velocity growth after some time, but with this particular time now depending on the wavelength.

However, even under the more sophisticated form that they consider, the constitutive law proposed by *Prakash and Clifton* [1993], in that it deals with moving surfaces, cannot be used as such for ABZ-like studies in which an event is nucleated by an externally applied normal stress component (the pore pressure) while the fault plane is at rest. Indeed, as can be seen on the simplified expression (6), the strength is assumed to be altered by the slip but not directly by the time since a normal stress change. The slip cannot be initiated in this way with this friction law.

To remedy to this problem, we use a modified version of the simplified Prakash-Clifton law, for which strength $\tau_1^s > 0$ at a given point on the fault also evolves with time following normal stress changes (see Figure 5) according to

$$\dot{\tau}_1^s = -\frac{|V| + V^\star}{L}[\tau_1^s - f \max(0, -\tau_2)] \ , \qquad (7)$$

where $V^\star$ is a positive constant and in which, similarly to Coulomb friction, it is understood that when $V = 0$, sliding is initiated when $|\tau_1|$ becomes equal to $\tau_1^s$, whereas $|\tau_1| = \tau_1^s$ during sliding, and $\tau_1 V \geq 0$ in all cases. The characteristic distance $L$ deduced from the Prakash and Clifton experiments, when fitted to an expression like (6), is of order microns, whereas when $V = 0$, the characteristic time of evolution to the new Coulomb strength following a change in normal stress, $L/V^\star$, would have to be determined by other experiments able to cope with this issue. It might be possible to deduce an upper bound for this time constant from the experiments by *Linker and Dieterich* [1992], in that it should be less than the shortest timescale that they are able to resolve in their experiment leading to the apparent instantaneous jump in normal stress that they report (see discussion in section 4.1). For the time being, however, and since we are mainly concerned with qualitative features, the constraints on how small the value of $L$ can be made are dictated by computational limitations. We simply ensure that $V^\star$ remains significantly smaller than representative seismic slip velocities, i.e., average slip velocities reached during well-developed ruptures (not dying pulses), the restriction in this matter being also dictated by computer limitations. As remarked, *Ranjith and Rice* [2000] showed that the conclusion that they draw concerning regularization of ill-posedness remains unchanged when using the modified expression (7).

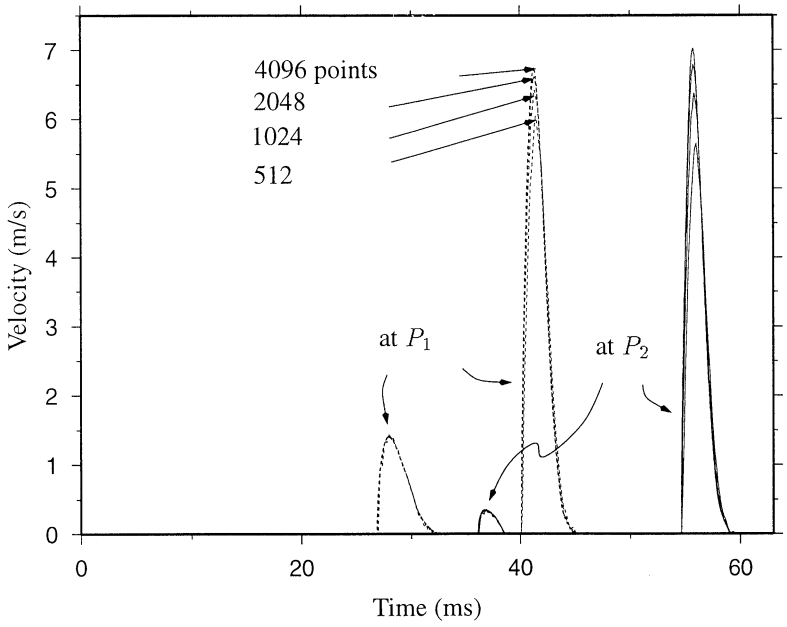


**Figure 6.** Same parameters as in Figure 3 (Adams unstable, generalized Rayleigh wave speed defined) but with the regularizing modified Prakash-Clifton law (equation (7) with $L = 8.5$ mm, $V^\star = 1$ m/s). Convergence through grid size reduction is obtained. The pulse is self-sustained and propagates nearly at the generalized Rayleigh wave speed in the direction of slip in the more compliant medium. Behavior is qualitatively similar in the Adams unstable range without a generalized Rayleigh wave speed (corresponding to case 2 in Figure 2), but the pulse's rupture velocity is essentially that of the slower S wave speed, in agreement with the *Ranjith and Rice* [2000] modal analysis. Depending on parameters, for decreasing values of the characteristic distance $L$, the peak velocity of the pulse grows faster with propagation distance. For increasing $L$, there is a transition above which the pulse dies.

While we have not attempted it yet in our work, we note that it should also be possible to do converging simulations based on the regularization of Coulomb friction of *Martins and Simões* [1995] and *Simões and Martins* [1998], in which local normal stress is replaced by its average over some finite area.

### 4.3. Well Resolved "Weertman" Pulses

We can now attempt to simulate the same conditions that led to ill-posedness with classical Coulomb friction. We again use the set of parameters used by ABZ and in Figure 3, but with friction law (7). Similarly to Figure 3, slip velocity as a function of time is shown in Figure 6 for different grid resolutions. We now have convergence through grid size reduction and can have some confidence in the validity of the solution. The rupture velocity $V_r$ of the pulse is determined by finding the points along the fault at which the disturbance begins for various times for the best resolution used. We find that the average rupture velocity between $P_1$ and $P_2$ is $V_r = 2414 \pm 5$ m/s. This velocity is less than and very close to the generalized Rayleigh wave speed which is $c_{GR} = 2474.56$ m/s in this case. We therefore refer to this as a "Weertman pulse" since *Weertman* [1980] suggested that such pulses could propagate at the generalized Rayleigh wave speed [see also *Adams*, 1998]. We see that the pulse is now self-sustained. The pulse does not split into two pulses, as had been reported in ABZ. Other results (not shown here) show that the width of the pulse decreases with increasing propagation distance. The velocity of the other (dying) pulse measured between $P_1$ and $P_2$ is $V_r = 4007 \pm 14$ m/s, which is close to the slower P wave speed of $c_p^+ = 4330$ m/s.

To give a more general view of the event, we present the spatiotemporal evolution of slip velocity in Figure 7 and a contour plot of the solution in Figure 8. We see a wide dying disturbance that propagates at a not well defined velocity between the P wave speeds in the negative $x_1$ direction as well as another dying pulse propagating at the slower P wave speed in the positive $x_1$ direction. Only the Weertman pulse is self-sustained, and it propagates in the positive $x_1$ direction with a velocity that is close to that of the generalized Rayleigh wave speed. In Figure 9 we also show the different fields as a function of time for the Weertman pulse at point $P_1$ (note that slip velocity was already presented in Figure 6).

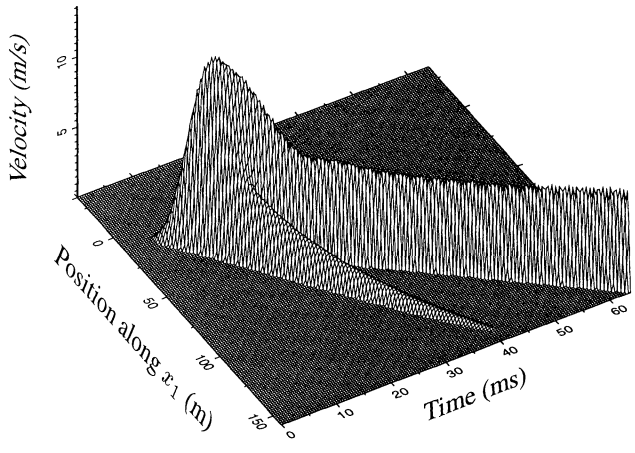


**Figure 7.** Space-time view of the Weertman pulse for the regularized formulation. Same parameters as in Figure 6; the best resolution was used ($N = 4096$).

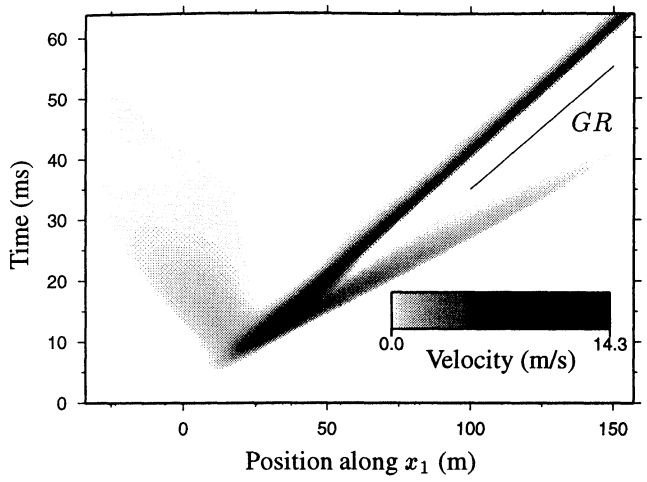


**Figure 8.** Similar to Figure 7; the propagating velocity of the Weertman pulse is close to that of the generalized Rayleigh wave speed. On this plot, the highest velocities are reached inside the nucleation region.

For conditions under which the generalized Rayleigh wave speed does not exist but still in the unstable range ($f > f_{\text{crit}}$), we get the same qualitative results as in Figures 6-8 except that the self-sustained pulse propagates at about the slower S wave speed. As expected, for conditions under which the generalized Rayleigh wave speed does not exist and in the stable range, we always find dying pulses, similar to what is shown in Figure 4.

### 4.4. A Self-Sustained Pulse in the Opposite Direction

So far the self-sustained pulses observed were all propagating in the positive $x_1$ direction, i.e., the direction of slip in the more compliant medium. This is the direction predicted by *Weertman* [1980] and later found in ABZ. However, in their stability analysis, as discussed previously, *Ranjith and Rice* [2000], extending *Adams* [1998] results, found that in some cases and for sufficiently high friction coefficient, other unstable modes exist. They propagate in the opposite direction, at a velocity a little more than the slower P wave, and are less unstable than the lower speed modes. (In retrospect, this new family of modes can also be found with Adams' method; they correspond to yet other curves in Figure 2 (top) (one for each material contrast), emerging at a higher value of the friction coefficient and remaining below the curve corresponding to the usual family of modes.) This suggests the possibility of self-sustained pulses propagating in the opposite direction in our model. For a 20% contrast, *Ranjith and Rice* [2000] found that the condition of existence of such modes is $f > 0.22$, so is should be possible to excite them in the ABZ case for which $f = 0.75$.

In Figure 10 we show the slip velocity at observation point $P_3$, and in Figure 11 we show a space-time view of slip ve-

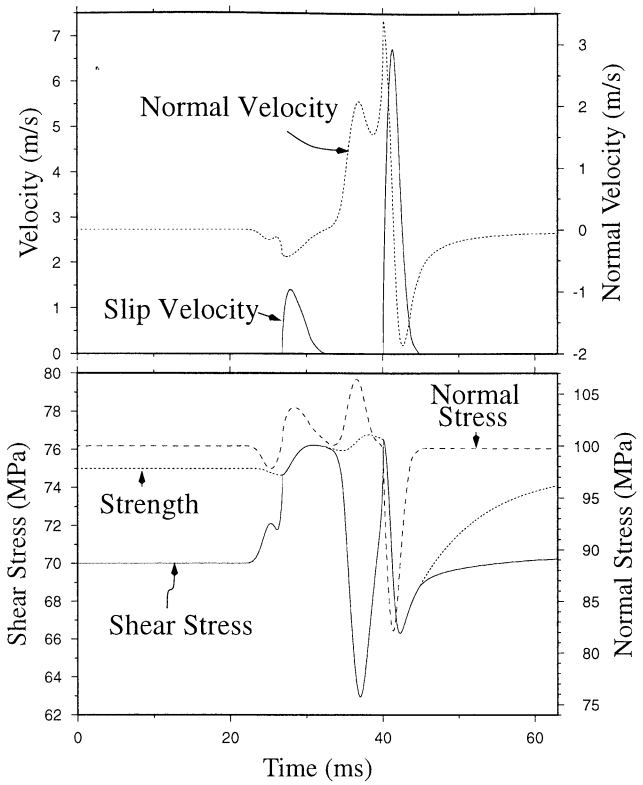


**Figure 9.** (top) Slip velocity (solid line) and normal velocity (dashed line). (bottom) Shear stress (solid line), shear strength (short-dashed line), and normal stress (long-dashed line), for the Weertman pulse at observation point $P_1$. Note that the normal velocity represents the velocity in the $x_2$ direction of both sides, i.e., there is no opening. (Same parameters as in Figure 7.)

locity, using a nucleating ellipse with velocity about equal to the slower P wave speed, propagating in the negative $x_1$-direction. Again, the pulse is well resolved numerically. Also note that the Weertman pulse is not excited in this case. Consistently with the *Ranjith and Rice* [2000] analysis, we found that this pulse is less favored than the Weertman pulse: we had to use a smaller value of $L$ in order to have a self-sustained (versus dying) pulse. Also, we have not been able to generate this pulse with a circular nucleation region, in contrast to the case of the Weertman pulse which can be generated this way (even if less vigorous, everything else being equal). Monitoring of the velocity of the pulse at various points shows that it increases from $V_r = 4218$ m/s near the origin to $V_r = 4301$ m/s, whereas the slower P wave speed is $c_p^+ = 4330$ m/s.

This opposite pulse was obtained under condition of existence of the generalized Rayleigh wave speed. When the generalized Rayleigh speed does not exist, the modal analysis shows a similar result. However, for the cases tested here (30% contrast), this new family of modes appear at a value rather irrelevant for seismology, i.e., $f > 1.75$.

At the present level of progress, we are unable to determine the precise limits to parameter ranges (material properties, friction, loading details) for which self-sustained pulses exist. Some elements of answers will be provided in the discussion.

## 5. Discussion and Conclusions

### 5.1. Summary

We have reproduced the *Andrews and Ben-Zion* [1997] (ABZ) study of simulations of ruptures along bimaterial interfaces under Coulomb friction. We have illustrated the ill-posed character of the problem for some parameter range; grid size reduction does not lead to convergence of the solutions. We show that an experimentally based friction law, which tends toward the Coulomb law for large slip or time, provides a regularization. With this new law, we find that the main (qualitative) conclusion of ABZ, namely, the existence of a self-sustained pulse, still holds. When the generalized Rayleigh wave speed exists, the pulse propagates essentially at that velocity in the direction of slip in the more compliant medium. As a slight extension of the ABZ results, it propagates at essentially the slower S wave speed and in the same direction, when the generalized Rayleigh wave speed is not defined. However, contrary to ABZ, we have not observed splitting of the pulses.

As anticipated from the *Ranjith and Rice* [2000] modal analysis, we find that another class of (less unstable) pulses can be generated. They propagate in the opposite direction, at a velocity close to the slower P wave speed.

In fact, we find that all our results (ill-posedness, propagation velocities, and growth rate of pulses) are consistent with the *Ranjith and Rice* [2000] analysis. Figure 12 illustrates the first two points and summarizes our mains findings.

### 5.2. Adams' Steady State Pulse

As briefly mentioned in section 1.2, with Coulomb friction and when the generalized Rayleigh wave speed exists, there exists a steady state propagating slip pulse solution [*Adams*, 1998; *Rice*, 1997]. The solution can, in fact, consist of a train of any number of pulses, but let us consider only one pulse, which is the case of interest here.

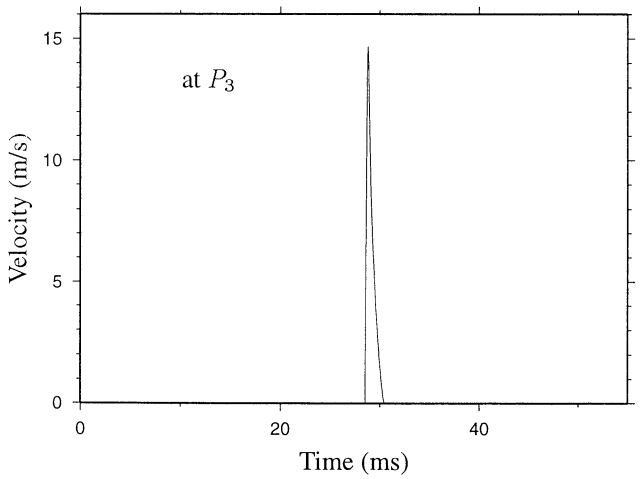


**Figure 10.** A pulse in the opposite direction. Consistently with the *Ranjith and Rice* [2000] stability analysis, we find that a self-sustained pulse can propagate in the direction opposed to that of the Weertman pulse. We show the slip velocity at observation point $P_3$ for a 20% material contrast, $f = 0.75$. (Same parameters as in Figure 6 except for $L = 2$ mm and $a_{\text{ell}} = 60$ m, $b_{\text{ell}} = 10$ m, and $v_{\text{ell}} = 4264$ m/s.)

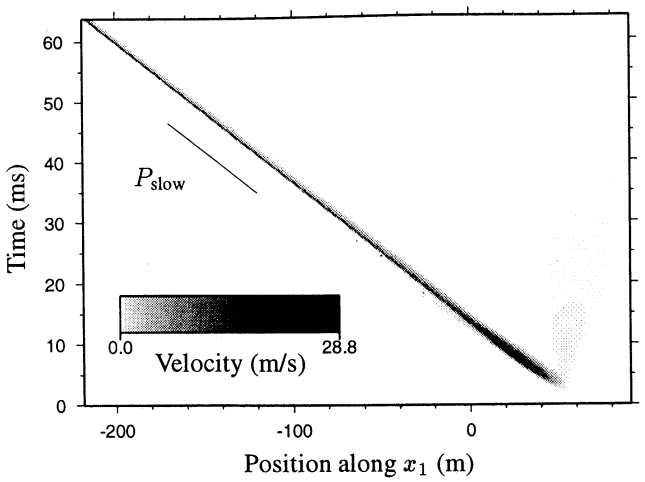


**Figure 11.** Same as Figure 10, space-time global view. Also in agreement with *Ranjith and Rice* [2000], we find that the velocity of propagation of this pulse is a little less than the slower P wave speed. On this plot, the highest velocities are reached within the leftmost portion of the pulse (and would keep on increasing).

In that solution the shear stress is uniform along the fault, equal to the initial one, $\tau_1^0$ (assumed smaller than the threshold $f|\tau_2^0|$). The compressive normal stress is equal to the initial one $|\tau_2^0|$ everywhere except within the pulse zone, in which it is uniform and equal to $|\tau_1^0|/f$. It is thus the reduction in normal stress that is the driving mechanism.

As the pulse is steady state, it is legitimate to speak about an apparent coefficient of friction $f^\star$, i.e., that which would be measured in a friction experiment. Here $f^\star = |\tau_1^0|/|\tau_2^0| < f$. In particular, one can have $f^\star = 0$, corresponding to a complete drop in normal stress. In other words, one can have sliding with an arbitrarily low initial shear stress and an arbitrarily high coefficient of friction $f$ but, e.g., without any generation of heat.

Within the pulse, of arbitrary risetime and propagating in the direction of motion in the softer medium at the generalized Rayleigh wave speed, the slip velocity is uniform, given by

$$V = \frac{(f|\tau_2^0| - \tau_1^0)c_{GR}}{f\mu^\star(c_{GR})} \tag{8}$$

where $\mu^\star(c)$ is a complicated function of speed $c$ and of material properties, given by *Weertman* [1980].

(There is a misprint in equation (11) of *Weertman* [1980] for $\mu^\star$, which makes it dimensionally inconsistent. The simplest way to restore dimensionality and have the required change of sign of $\mu^\star$ upon switching materials provides the correct expression, which we have checked independently to be (in the notation of *Weertman* [1980])

$$\mu^\star = \frac{2\mu_1\mu_2}{\Delta}[\mu_1(\gamma_1\beta_1 - \alpha_1^4)(\gamma_2\beta_2 - \alpha_2^2) - \mu_2(\gamma_2\beta_2 - \alpha_2^4)(\gamma_1\beta_1 - \alpha_1^2)] . \tag{9}$$

For completness, we also recall the expression for $\bar{\mu}$ (equation (2) of *Weertman* [1980]), which provides the value of $c = c_{GR}$ when $\bar{\mu}(c) = 0$:

$$\bar{\mu} = \frac{2\mu_1\mu_2}{\Delta}[\mu_1\gamma_2(1-\alpha_2^2)(\gamma_1\beta_1 - \alpha_1^4) + \mu_2\gamma_1(1-\alpha_1^2)(\gamma_2\beta_2 - \alpha_2^4)] . \tag{10}$$

Here $\alpha_i = \sqrt{1 - c^2/2c_{si}^2}$, $\beta_i = \sqrt{1 - c^2/c_{si}^2}$ and $\gamma_i = \sqrt{1 - c^2/c_{pi}^2}$, with $i = 1$ or 2, while $\Delta$, which is given as equation (3) of *Weertman* [1980], can be rewritten in the more compact but equivalent form

$$\Delta = \mu_1^2(1-\gamma_2\beta_2)(\gamma_1\beta_1 - \alpha_1^4) + \mu_2^2(1-\gamma_1\beta_1)(\gamma_2\beta_2 - \alpha_2^4) + \mu_1\mu_2[(1-\alpha_1^2)(1-\alpha_2^2)(\gamma_1\beta_2 + \gamma_2\beta_1) + 2(\gamma_1\beta_1 - \alpha_1^2)(\gamma_2\beta_2 - \alpha_2^2)] . \tag{11}$$

The subscripts '1' and '2' in the above expressions correspond to our plus and minus superscripts, respectively. The curves in Figures 1 and 2 of *Weertman* [1980] have been obtained with the correct expression for $\mu^\star$ and, noting that ABZ used a convention for subscripts '1' and '2' opposite to that of *Weertman* [1980], their Figure 4 provides the proper representation of $\mu^\star$ and $\bar{\mu}$ for the 20% material contrast that we use in this paper.)

It seems that the steady state *Adams* [1998] pulse could not be stable to perturbation (due to the *Adams* [1995] instability) and could not emerge from generic initial conditions; it may, indeed, have a vanishing basin of attraction.

### 5.3. Influence of Parameters

A very limited exploration of parameter space has been performed. It is clear (and not surprising) that effects of the various parameters are strongly coupled. For example, it has been observed that, for some parameters, a nucleation region with $a_{ell} = b_{ell} = 60$ m (i.e., circular space-time nucleation process, $v_{ell}$ being then irrelevant) leads to a dying pulse while the naively weaker $a_{ell} = 10$ m, $b_{ell} = 60$ m leads to a self-sustained pulse, everything else being equal. Nevertheless, in general, some features are relatively robust.

**5.3.1. Effect of initial stresses.** We observe that the lower $|\tau_1^0|$, the harder it is for an event to be initiated, which is the expected behavior. For the conditions we tried, no self-sustained pulse could be nucleated for $|\tau_1^0|$ less than $\sim 90\%$ of $f|\tau_2^0|$.

Equation (8) shows that for the idealized steady state Adams pulse the lower $|\tau_1^0|$, the higher slip velocity. Shear stress is not altered at all during propagation. Instead, the driving mechanism is the drop of normal stress that occurs within the pulse, to such a level that the (unaltered) shear stress meets the Coulomb condition. Hence, such a self-sustained pulse may exist even with zero shear stress (however, the slip velocities thus generated would be significantly higher than what is generally believed: formula (8) with $\tau_1^0 = 0$ gives $V \sim 55$ m/s at a 10 km depth under hydrostatic

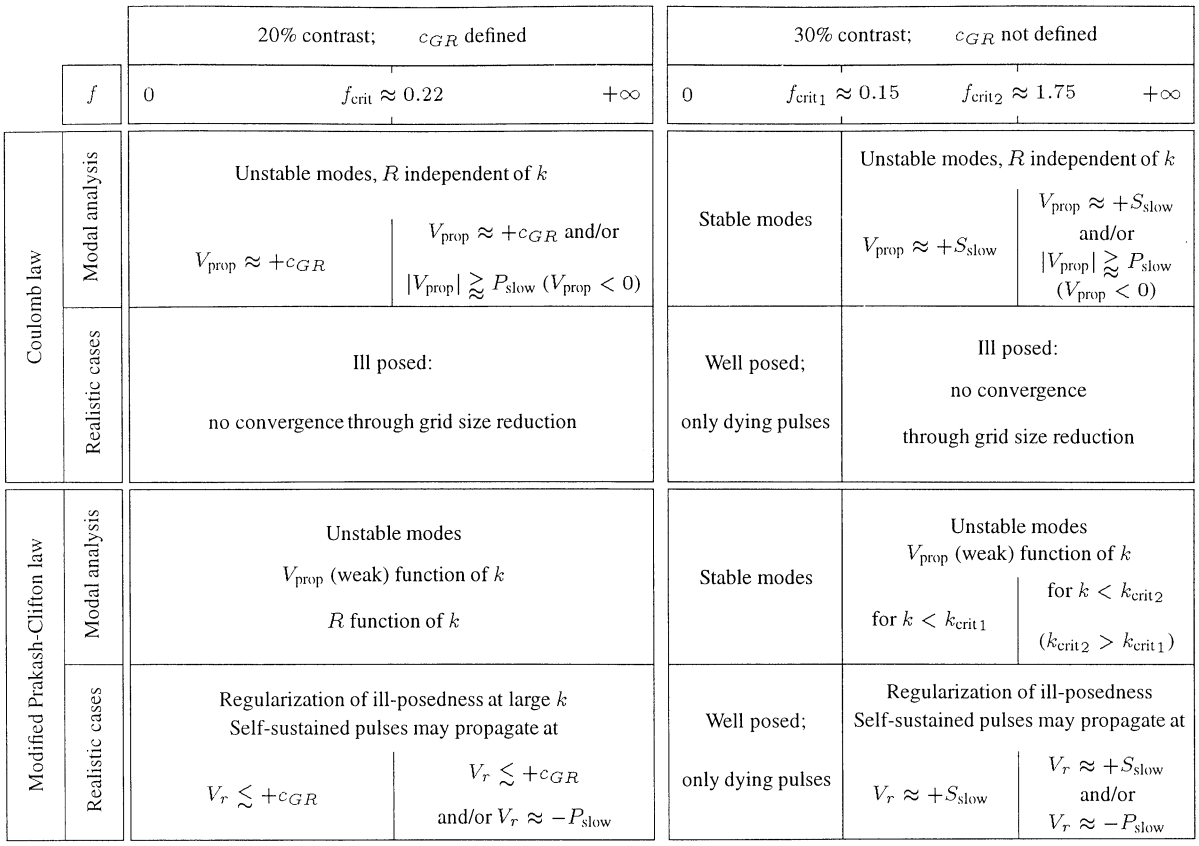


**Figure 12.** Summary of results, with link to *Ranjith and Rice* [2000] modal analysis. $R$ is normalized growth rate (see Figure 2); $k$ is mode number; $V_{\text{prop}}$ is propagation velocity of harmonic modes; $V_r$ is propagation velocity of pulses in simulations like reported here. Sign of propagation velocities refers to the direction of propagation, plus being that of the direction of slip in the more compliant medium, minus being the opposite direction. Note the closeness between the theoretical $V_{\text{prop}}$ for the Coulomb law and the numerically observed $V_r$ for simulations that have been made possible through the regularization with the Prakash-Clifton law.

pressure for a 20% material contrast). With this idealized pulse the static and dynamic shear stress drops are exactly zero. Figure 9 shows that the static one is very close to zero in the simulations. Although the minimum possible value of compressive normal stress $-\tau_2$ within the slipping region for the Adams steady pulse solution is zero (occurs in limit of zero shear stress) and there is no opening, it may be that for pulses of growing amplitude, there is complete normal stress reduction followed by opening. Such response is hinted at by results of ABZ and by some of our own results, although it cannot be resolved at the present level of our modeling, not least because we have disallowed the opening degree of freedom included in the general *Breitenfeld and Geubelle* [1998] numerical methodology. Further analysis might thus invalidate the argument that opening is precluded for earthquake ruptures because of high normal pressure.

However, in all simulations performed so far, reducing $|\tau_1^0|$ has the more classical effect of diminishing slip velocity. For the pulses that are self-sustained and look almost steady state (like that in Figure 6) it is observed that that the variation of shear stress within the pulse decreases with increasing distance, while the variation of normal stress increases. This suggests that the pulse might be approaching the theoretical steady state pulse, but if it is so, it is still too far from it for the expected relation between initial shear stress and slip velocity to be verified (formula (8) gives $V \sim 2$ m/s) for the parameters of Figure 6 while the observed slip velocity is $\sim 7$ m/s). In fact, the nucleation procedure that we used, with total drop in normal stress in the nucleation region, creates a very large drop in shear stress. So the initial conditions are already far from the idealized steady state pulse. More simulations, with different nucleation procedures, will be necessary to understand this issue.

**5.3.2. Effect of the characteristic distance $L$.** For a given nucleation region size, and a given nucleation process by the pore pressure procedure described, $L$ controls whether the pulse decays or grows (i.e., is self-sustained). There is a transition value of $L$ below which the pulse will become self-sustained. Not surprisingly, the transitional value is smaller for lower initial shear stress. Also, below the critical value (i.e., for growing pulses) the rate of growth is lower for larger $L$, and this effect is much more pronounced for lower initial shear stress (for a given initial normal stress). That is, for a high initial shear stress a large alteration of $L$ (below the crit-

ical value) has little effect on the rate of growth of the pulse. Probably closely related is the effect of $L$ on the rupture velocity: larger $L$ implies slower $V_r$. The most visible effect of $L$ is on the width of the pulse.

**5.3.3. Width of pulses.** For self-sustained pulses, e.g., like in Figure 7, we observe that width (or, equivalently, risetime $T_r$) decreases slowly and slip increases slowly with propagation distance. For the limited parameter space exploration accomplished so far, $T_r$ seems to be mainly controlled by the characteristic distance in the friction law $L$ and by the risetime $T_\nu$ of the artificial nucleation process (i.e., not its total duration). This is given by $T_\nu = 2\,a_{\text{ell}}b_{\text{ell}}/(v_{\text{ell}}\sqrt{a_{\text{ell}}^2 + b_{\text{ell}}^2})$ (notation of Appendix B), or approximately $2\,a_{\text{ell}}/v_{\text{ell}}$ when $b_{\text{ell}} \gg a_{\text{ell}}$ as for Figures 6-9. For larger $T_\nu$ or larger $L$, $T_r$ is larger. In fact, the following observations suggest that the risetime will in the end be determined by $L$ alone (in some dimensionally consistent form like $\mu L/[c_{GR}(f|\tau_2^0| - \tau_1^0)]$). For large $T_\nu$ and small $L$, $T_r$ for the entire pulse width seems to be directly determined by $T_\nu$. However, the shape of the velocity pulse becomes very narrow for large values of $V$, as if its width tends to scale with $L$ even while the entire width is still influenced by the nucleation process. Consistently, $T_r$ decreases relatively rapidly with propagation distance. By contrast, when $T_\nu$ is small but $L$ is relatively large, one can have $T_r$ even greater than $T_\nu$ and the decrease of $T_r$ is not observable. This is still very speculative, and more studies are needed.

### 5.4. Observations

**5.4.1. Slip pulses in homogeneous media.** As mentioned in section 1, we now discuss a possible mechanism for explaining some features observed in homogeneous media. As an in-plane slip rupture propagates along a fault between initially identical solids, extensional fault-parallel strains are induced on the side of the fault and compressional strains on the other. It seems possible in sufficiently nonlinear materials that the moduli governing further increments of deformation could be affected by those strains, such that different incremental moduli would apply on one side of the fault than on the other. This nonlinear effect might make local response near the rupture tip mimic the linear response of dissimilar materials, such that nonuniform slip induces significant alterations of normal stress. Such is beyond our capabilities to address rigorously here but deserves attention since it may be the origin of the pulse-like ruptures, with local normal stress reduction and even fault opening, observed for fault propagation between foam rubber blocks by *Brune et al.* [1993]. This line of explanation, still speculative, ties the normal stress alterations in the foam rubber experiments to the strong nonlinearity of that material. Foam rubber is elastically more compliant in compression than in extension because load is carried by fibrils which readily buckle when compressed [*Gibson and Ashby*, 1999]. Thus the zone of reduced wave speeds would occur on the compressional side of the slip surface near the propagating tip. This is consistent with pulse propagation in the direction of slip in the material of slower wave speeds. Competent rock may be expected to be less susceptible to such effects (if they exist at all). The highly cracked and faulted zones bordering major faults [e.g., *Chester et al.*, 1993] may make those zones strongly nonlinear in their response to fault-parallel extensional and compressional straining. However, in this case we expect (because of crack closure under compression) the compressed side of the rupture to have increased incremental moduli and wave speeds, and that would not obviously be consistent with pulse generation in initially identical half-spaces with local crack/fault damage near their sliding borders (note that foam rubber-like rupture response has not been confirmed in laboratory rock experiments).

**5.4.2. Evidence of bimaterial effects for earthquakes?** Recently, *Rubin and Gillard* [2000] studied several thousand pairs of consecutive earthquakes which occurred on a segment of the central San Andreas fault, south of the Loma Prieta rupture. Among the second events of each pair which occurred close to the first one, i.e., within two radii ($\sim$ 200 events), they find that over 70% more occur to the northwest than to the southeast (at a larger distance, the distribution is roughly symmetric). They interpret this asymmetry as resulting from the contrast in material properties that exists at this location of the San Andreas fault, the medium being more compliant northeast of the fault than southwest [e.g., *Eberhart-Phillips and Michael*, 1998]. With this dissymmetry a Weertman pulse would propagate to the southeast. The *Rubin and Gillard* [2000] argument is twofold: first, an earthquake propagating to the southeast will receive an extra dynamic "kick," which means that the barriers ultimately stopping the rupture will be, on average, stronger at the southeastern end than at the northwestern one; second, after the rupture, the static shear and normal stresses outside the rupture zone are approximately symmetric (this is from *Weertman* [1980] and confirmed in our numerical simulations). The next rupture is then more likely to start at the northwest. (Note that the above reasoning does not consider the less likely "opposite" pulses discussed in section 4.4, which could in fact be responsible for part of the 30% remaining earthquakes.) *Rubin and Gillard* [2000] also present more direct evidence of preferential rupture propagation to the southeast by measuring pulse widths as a function of azimuth, but on an, of course, more limited number of events.

### 5.5. Further Work

An important point is that the mechanism discussed in this paper acts for in-plane but not for antiplane slip, since the latter causes no alteration of normal stress and hence provides no basis for unstable slippage when the Coulomb law is used. Thus what will happen in 3-D for, say, a rupture nucleated on a circular disc area along a bimaterial interface remains uncertain; there will two rupture edges with in-plane slip, conducive to the mechanism, but also two with antiplane slip.

Another unanswered question is to determine the behavior of the model with realistic nucleations under low overall shear stresses. As seen in section 5.3.1, it seems difficult to nucleate an event under only moderately low initial shear stress (an issue not specific to bimaterials). However, it remains to be determined what would happen for a

well-developed rupture (pulse or crack) entering a region of low shear stress in a bimaterial environment (it would be expected to die in a homogeneous medium, as that would be a relaxation barrier).

It also remains to be determined what controls precisely the width of a pulse and, more generally, what conditions lead to a self-sustained pulse. Future studies will have to consider opening, with an appropriate constitutive relationship yet to be determined.

## Appendix A: Numerical Method

The functionals $\phi_\alpha^\pm$ ($\alpha = 1, 2$) in the elastodynamic relations (1) can be written as

$$\phi_\alpha^\pm(x_1, t) = \frac{1}{2\pi}\int_{-\infty}^{+\infty} \Phi_\alpha^\pm(k, t) e^{ikx_1} dk \,, \tag{A1}$$

where the Fourier coefficients $\Phi_\alpha^\pm$ are related to the Fourier coefficient $U_\alpha^\pm$ of displacement $u_\alpha^\pm$ through a linear combination of convolution integrals, namely,

$$\Phi_\alpha^\pm(k, t) = \sum_{\beta=1}^{2} C_{\alpha\beta}^\pm \int_0^t H_{\alpha\beta}(|k| c_s^\pm t') U_\beta^\pm(k, t - t') dt' \,, \tag{A2}$$

which makes clear the coupling between the two possible rupture modes in this problem (I and II). The expressions for the convolution kernels $H$ are given by *Breitenfeld and Geubelle* [1998] in the Laplace domain. (We note that the signs of each first term of each first equation of equations (4) and (6) of *Breitenfeld and Geubelle* [1998] should both be $\mp$ instead of $-$ and $\pm$, respectively.) Out of the three different kernels ($H_{12} = H_{21}$), *Breitenfeld and Geubelle* [1998] were able to derive analytical expressions in the time domain for only two of them and some integrals would still have to be computed numerically. So we found it more convenient to compute all three kernels by numerical inversion of Laplace transforms. This operation appears to be a delicate thing to do, at least for the Bessel-like expressions that we have to deal with. We tried several commercial and noncommercial routines, but the only one which was always satisfactory was that by *Honig and Hirdes* [1984]. Each kernel has to be derived only once and is stored in a file for tabulated values of the argument, and later interpolated at the required values.

For numerical treatments we write the displacement and the functionals as the truncated Fourier series:

$$\begin{Bmatrix} u_\alpha^\pm(x_1, t) \\ \phi_\alpha^\pm(x_1, t) \end{Bmatrix} = \sum_{j=-N/2}^{N/2} \begin{Bmatrix} U_\alpha^\pm(k_j, t) \\ \Phi_\alpha^\pm(k_j, t) \end{Bmatrix} e^{ik_j x_1} \,, \tag{A3}$$

where $N$ is some large even number, $k_j = 2\pi j/\lambda$, $\lambda$ being some replication length along the $x_1$ axis. Finally, we use a fully explicit time marching scheme and find that, as suggested by *Breitenfeld and Geubelle* [1998], taking $h = \max(c_s^+, c_s^-)\Delta t/\Delta x_1 = 0.4$ seems to be a very good compromise for stability, accuracy, and efficiency (the value of $h$ expressed in terms of the P wave velocities is simply that just given times $\sqrt{2(1-\nu)/(1-2\nu)}$, namely, $\sqrt{3}$ for a Poissonian solid as used in this paper.

The method described above has been referred to as "independent" by *Breitenfeld and Geubelle* [1998] because it involves the displacements of both sides of the interface, by contrast to that named the "combined" method which deals with the relative displacements. As noted by *Breitenfeld and Geubelle* [1998], the independent method appears more stable for a given value of $N$. For the combined method the required memory is half, there are fewer convolution integrals (as in A2) to compute, and, furthermore, the method without replication of *Cochard and Rice* [1997] can be applied, which is not the case here (here we, of course, use a domain large enough to avoid influence of replications during the time for which results are shown).

## Appendix B: Event Nucleation by an Imposed Pore Fluid Pressure

The events in our simulations are nucleated by artificially prescribing fluid pressure in an elliptical region of the $x_1 - t$ plane. The following expressions are directly adapted from ABZ. The following coordinates are used:

$$\begin{aligned} \xi &= (x_1 - v_{\text{ell}} t)/a_{\text{ell}} \\ \eta &= (x_1 + v_{\text{ell}} t)/b_{\text{ell}} - \eta_0 \end{aligned} \tag{B1}$$

with $\eta_0 = \sqrt{a_{\text{ell}}^2 + b_{\text{ell}}^2}/b_{\text{ell}}$. The boundary of the pressure source is the ellipse of equation

$$1 - \xi^2 - \eta^2 = 0 \,. \tag{B2}$$

Within this elliptical domain the pore fluid pressure is given by

$$P_f = P_0(1 - \xi^2 - \eta^2)^2 \,, \tag{B3}$$

while it is zero outside. Thus it rises smoothly from 0 to $P_0$ at the center of the ellipse. For $a_{\text{ell}}$ significantly smaller than $b_{\text{ell}}$ this source looks like a disturbance roughly propagating at velocity $v_{\text{ell}}$ for $v_{\text{ell}} > 0$ (more precisely, the locus of maximum pressure propagates at a velocity a little less than $v_{\text{ell}}$). The shape and orientation of the ellipse can be seen in Figure 9 of ABZ and can be inferred from, e.g., our Figure 8 where $a_{\text{ell}} = 10$ m, $b_{\text{ell}} = 60$ m, and $v_{\text{ell}} = 2475$ m/s. For all the simulations presented in this paper we use $P_0 = |\tau_2^0| = 100$ MPa, where $|\tau_2^0|$ is the external, uniform, normal stress, so that full drop in normal stress is reached at the center of the nucleation region (when $P_f = P_0$).

**Acknowledgments.** This study was supported by the Southern California Earthquake Center (SCEC), by USGS grant 99-HQ-GR-0025 to Harvard University, and by a Blaise Pascal International Research Chair of the Foundation of École Normale Supérieure, Paris, to J.R.R., with additional support from the Office of Naval Research grant N00014-96-10777 to Harvard. SCEC is supported by NSF Cooperative Agreement EAR-8920136 and USGS Cooperative Agreement 1434-HQ-97-AG-01718. Discussions with Rachel Abercrombie, Joe Andrews, Yehuda Ben-Zion, Lionel Bureau, Tristan Baumberger, Christiane Caroli, Rodney Clifton, Steve Day, Philippe Geubelle, Ruth Harris, Raúl Madariaga, and Allan

Rubin, as well as with our coworkers K. Ranjith and Nadia Lapusta, are greatly acknowledged. We are also extremely grateful to George Adams for providing his Fortran codes, used to generate Figure 2, and again to K. Ranjith for urging study showing existence of the P wave pulse (section 4.4). Finally, reviews by J. Andrews, Y. Ben-Zion, and Eliza Richardson helped us to improve the presentation and clarify some issues.

## References

Achenbach, J. D., and H. I. Epstein, Dynamic interaction of a layer and a half-space, *J. Eng. Mech. Div., EM5*, 27–42, 1967.

Adams, G. G., Self-excited oscillations of two elastic half-spaces sliding with a constant coefficient of friction, *J. Appl. Mech., 62*, 867–872, 1995.

Adams, G. G., Steady sliding of two elastic half-spaces with friction reduction due to interface stick-slip, *J. Appl. Mech., 65*, 470–475, 1998.

Andrews, D. J., and Y. Ben-Zion, Wrinkle-like slip pulse on a fault between different materials, *J. Geophys. Res., 102*, 553–571, 1997.

Beeler, N. M., and T. E. Tullis, Self-healing slip pulses in dynamic rupture models due to velocity-dependent strength, *Bull. Seismol. Soc. Am., 86*, 1130–1148, 1996.

Ben-Zion, Y., Properties of seismic fault zone waves and their utility for imaging low-velocity structures, *J. Geophys. Res., 103*, 12,567–12,585, 1998.

Ben-Zion, Y., and D. J. Andrews, Properties and implications of dynamic rupture along a material interface, *Bull. Seismol. Soc. Am., 88*, 1085–1094, 1998.

Beroza, G. C., and T. Mikumo, Short slip duration in dynamic rupture in the presence of heterogeneous fault properties, *J. Geophys. Res., 101*, 22,449–22,460, 1996.

Bouchon, M., and D. Streiff, Propagation of a shear crack on a nonplanar fault: A method of calculation, *Bull. Seismol. Soc. Am., 87*, 61–66, 1997.

Breitenfeld, M. S., and P. H. Geubelle, Numerical analysis of dynamic debonding under 2D in-plane and 3D loading, *Int. J. Fract., 93*, 13–38, 1998.

Brune, J. N., S. Brown, and P. A. Johnson, Rupture mechanism and interface separation in foam ruber models of earthquakes: A possible solution to the heat flow paradox and the paradox of large overthrusts, *Tectonophysics, 218*, 59–67, 1993.

Bureau, L., T. Baumberger, and C. Caroli, Shear response of a frictional interface to a normal load modulation, *Phys. Rev. E*, in press, 2000.

Chester, F. M., J. P. Evans, and R. L. Biegel, Internal structure and weakening mechanisms of the San Andreas Fault, *J. Geophys. Res., 98*, 771–786, 1993.

Cochard, A., and R. Madariaga, Dynamic faulting under rate-dependent friction, *Pure Appl. Geophys., 142*, 419–445, 1994.

Cochard, A., and R. Madariaga, Complexity of seismicity due to highly rate dependent friction, *J. Geophys. Res., 101*, 25,321–25,336, 1996.

Cochard, A., and J. R. Rice, A spectral method for numerical elastodynamic fracture analysis without spatial replication of the rupture event, *J. Mech. Phys. Solids, 45*, 1393–1418, 1997.

Day, S. M., Three-dimensional finite difference simulation of fault dynamics: Rectangular faults with fixed rupture velocity, *Bull. Seismol. Soc. Am., 72*, 705–727, 1982.

Eberhart-Phillips, D., and A. J. Michael, Seismotectonics of the Loma Prieta, California, region determined from three-dimensional $v_p$, $v_p/v_s$, and seismicity, *J. Geophys. Res., 103*, 21,099–21,120, 1998.

Feng, R., and T. V. McEvilly, Interpretation of seismic reflection profiling data for the structure of the San Andreas fault zone, *Bull. Seismol. Soc. Am., 73*, 1701–1720, 1983.

Geubelle, P. H., and J. R. Rice, A spectral method for three-dimensional elastodynamic fracture problems, *J. Mech. Phys. Solids, 43*, 1791–1824, 1995.

Gibson, L. J., and M. F. Ashby, *Cellular Solids: Structure and Properties*, 2nd ed., Cambridge Univ. Press, New-York, 1999.

Harris, R. A., and S. M. Day, Dynamics of fault interaction: Parallel strike-slip faults, *J. Geophys. Res., 98*, 4461–4472, 1993.

Harris, R. A., and S. M. Day, Effect of a low-velocity zone on a dynamic rupture, *Bull. Seismol. Soc. Am., 87*, 1267–1280, 1997.

Heaton, T. H., Evidence for and implications of self-healing pulses of slip in earthquake rupture, *Phys. Earth Planet. Inter., 64*, 1–20, 1990.

Honig, G., and U. Hirdes, A method for the numerical inversion of Laplace transforms, *J. Comput. Appl. Math., 10*, 113–132, 1984.

Johnson, E., On the initiation of unidirectional slip, *Geophys. J. Int., 101*, 125–132, 1990.

Johnson, E., The influence of the lithospheric thickness on bilateral slip, *Geophys. J. Int., 108*, 151–160, 1992.

Lachenbruch, A. H., and J. H. Sass, Heat flow and energetics of the San Andreas fault zone, *J. Geophys. Res., 85*, 6185–6222, 1980.

Li, Y.-G., K. Aki, D. Adams, A. Hasemi, and H. K. Lee, Seismic guided waves trapped in the fault zone of the Landers, California, earthquake of 1992, *J. Geophys. Res., 99*, 11,705–11,722, 1994.

Linker, M. F., and J. H. Dieterich, Effects of variable normal stress on rock friction: Observations and constitutive equations, *J. Geophys. Res., 97*, 4923–4940, 1992.

Lippmann, H., Mechanics of bumps in coal mines: A discussion of violent deformations in the sides of roadways in coal seams, *Appl. Mech. Rev., 40*, 1033–1043, 1987.

Lomnitz-Adler, J., Model for steady state friction, *J. Geophys. Res., 96*, 6121–6131, 1991.

Magistrale, H., and C. Sanders, P-wave image of the Peninsular Ranges batholith, southern California, *Geophys. Res. Lett., 22*, 2549–2552, 1995.

Martins, J. A. C., and F. M. F. Simões, On some sources of instability/ill-posedness in elasticity problems with Coulomb's friction, in *Contact mechanics*, edited by M. Raous, M. Jean, and J. J. Moreau, pp. 95–106, Plenum, New York, 1995.

Mora, P., and D. Place, Simulation of the frictional stick-slip instability, *Pure Appl. Geophys., 143*, 61–87, 1994.

Oglesby, D. D., R. J. Archuleta, and S. B. Nielsen, earthquakes on dipping faults: The effects of broken symmetry, *Science, 280*, 1055–1059, 1998.

Olsen, K. B., R. Madariaga, and R. J. Archuleta, Three-dimensional dynamic simulation of the 1992 Landers earthquake, *Science, 278*, 834–838, 1997.

Perrin, G., J. R. Rice, and G. Zheng, Self-healing slip pulse on a frictional surface, *J. Mech. Phys. Solids, 43*, 1461–1495, 1995.

Prakash, V., Frictional response of sliding interfaces subjected to time varying normal pressures, *J. of Tribol., 120*, 97–102, 1998.

Prakash, V., and R. J. Clifton, Time resolved dynamic friction measurements in pressure-shear, in *Experimental Techniques in the Dynamics of Deformable Solids*, edited by K. T. Ramesh, *AMD* vol. 165, pp. 33–48, Appl. Mech. Div., ASME, New York, 1993.

Ranjith, K., and J. R. Rice, Slip dynamics at an interface between dissimilar materials, *J. Mech. Phys. Solids*, in press, 2000.

Renardy, M., Ill-posedness at the boundary for elastic solids sliding under Coulomb friction, *J. of Elasticity, 27*, 281–287, 1992.

Rice, J. R., Slip pulse at low driving stress along a frictional fault between dissimilar media, *Eos Trans. AGU, 78(46)*, Fall Meet. Suppl., F464, 1997.

Richardson, E., and C. Marone, Effects of normal stress vibrations on frictional heating, *J. Geophys. Res., 104*, 28,859–28,878, 1999.

Rubin, A. M., and D. Gillard, Aftershock asymmetry/rupture directivity among central San Andreas fault microearthquakes, *J. Geophys. Res., 105*, 19,095–19,109, 2000.

Simões, F. M. F., and J. A. C. Martins, Instability and ill-posedness in some friction problems, *Int. J. Eng. Sci., 36*, 1265–1293, 1998.

Weertman, J. J., Dislocations moving uniformly on the interface between isotropic media of different elastic properties, *J. Mech. Phys. Solids, 11*, 197–204, 1963.

Weertman, J. J., Unstable slippage across a fault that separates elas-

tic media of different elastic constants, *J. Geophys. Res.*, *85*, 1455–1461, 1980.

York, G., and T. Dede, Plane strain numerical modelling of mining induced seismicity through the effects of mine geometry, backfill and dyke material, on tabular reefs at great depth, in *Rockbursts and Seismicity in Mines*, edited by S. J. Gibowicz and S. Lasocki, pp. 167–172, A. A. Balkema, Brookfield, Vt., 1997.

Zheng, G., and J. R. Rice, Conditions under which velocity-weakening friction allows a self-healing versus a cracklike mode of rupture, *Bull. Seismol. Soc. Am.*, *88*, 1466–1483, 1998.

Zoback, M. D., et al., New evidence on the state of stress on the San Andreas fault system, *Science*, *238*, 1105–1111, 1987.

A. Cochard, Laboratoire de Géologie, Ecole Normale Supérieure, 24, rue Lhomond, 75231 Paris Cedex 05, France. (cochard@geologie.ens.fr)

J. R. Rice, Division of Engineering and Applied Sciences, Harvard University, 29 Oxford Street, Cambridge, MA 02138. (rice@esag.harvard.edu)

(Received February 22, 2000; accepted June 14, 2000.)